Improving MODIS Surface BRDF/Albedo Retrieval With MISR Multiangle Observations

Yufang Jin, Feng Gao, *Member, IEEE*, Crystal B. Schaaf, *Member, IEEE*, Xiaowen Li, Alan H. Strahler, *Member, IEEE*, Carol J. Bruegge, and John V. Martonchik, *Associate Member, IEEE*

***Abstract*—We explore a synergistic approach to use the complementary angular samplings from the Multi-angle Imaging SpectroRadiometer (MISR) and Moderate Resolution Imaging Spectroradiometer (MODIS) to improve MODIS surface bidirectional reflectance distribution function (BRDF) and albedo retrieval. Preliminary case studies show that MODIS and MISR surface bidirectional reflectance factors (BRFs) are generally comparable in the green, red, and near infrared. An information index is introduced to characterize the information content of directional samplings, and it is found that MISR angular observations can bring additional information to the MODIS retrieval, especially when the MISR observations are close to the principal plane. We use the BRDF parameters derived from the MISR surface BRFs as *a priori* information and derive *a posteriori* estimates of surface BRDF parameters with the MODIS observations. Results show that adding MISR angular samplings can reduce the relative BRF prediction error by up to 10% in the red and green, compared to the retrievals from MODIS-only observations which are close to the cross-principal plane.**

***Index Terms*—Albedo, Earth Observing System (EOS), Moderate Resolution Imaging Spectroradiometer (MODIS), Multiangle Imaging SpectroRadiometer (MISR), remote sensing, surface bidirectional reflectance.**

I. Introduction

THE bidirectional reflectance distribution function (BRDF) characterizes the anisotropy of surface reflectivity [1], [2]. It has been used to normalize satellite measurements into a common sun–view geometry [3], to perform coupled atmospheric correction [4], and to derive canopy structure and other biogeophysical parameters [5]–[7]. The operational Moderate Resolution Imaging Spectroradiometer (MODIS) BRDF/albedo retrieval algorithm [8], [9] uses a three-parameter semiempirical RossThick–LiSparse–Reciprocal (RTLSR) BRDF model to capture the directionality of surface reflectance. The RTLSR model consists of two kernel-driven terms and a constant term. The volumetric kernel represents the scattering properties of turbid medium [10], and the geometric-optical kernel captures the shadowing effect of sparse vegetation [11], [12]. The constant term is added to represent the isotropic scattering. Validation with both field measurements and satellite observations has shown the capability of the RTLSR model to represent the shapes of naturally occurring BRDFs and its accuracy of predicting the reflectances [13]–[15].

One major concern in performing the BRDF inversion is the sparse angular sampling available from an individual sensor [16]. Remote sensing signals are usually correlated to some degree [17], and therefore not only the number of directions but also the diversity of angular samples should be large enough to ensure an overdetermined inversion. The volumetric and geometric kernels of the RTLSR model may not be completely orthogonal under some sampling conditions [18], which affects the stability of BRDF retrieval and its noise magnification [19], [20]. The analysis with field measurements of directional reflectances [13] has demonstrated that most empirical and semiempirical BRDF models can be inverted very well with sufficient and well-distributed measurements, but problems occur in situations of sparse sampling.

The acquisition of angular measurements from an individual sensor is limited by its scanning configuration and the platform's orbital characteristics [21]. Moreover, cloud contamination reduces the number of clear-sky observations and makes the angular distribution hard to predict. However, more complete angular samplings can be obtained by combining the observations from various sensors with complementary sampling characteristics. MODIS–Terra and MISR, both on board the Earth Observing System (EOS) Terra platform, for example, complement each other in the azimuth dimension. Using surface directional reflectances simulated by a canopy radiative transfer model [10], Lucht and Lewis [22] found that combining MODIS and MISR angular samplings can reduce the uncertainty and random noise amplification of BRDF/albedo retrievals [18]. However, we must recognize that the specific satellite spatial scale and noise must be accounted for when using actual remotely sensed data [13].

The high calibration quality and geolocation accuracy of both MODIS and MISR instruments [23], [24] and the similarity of their spectral bands in the visible and near infrared enhance the ability to perform data fusion of surface bidirectional reflectance factors (BRFs) from these two sensors [25], [26]. Operationally, however, additional noise may still be introduced due to the differences in spectral response functions, atmospheric correction schemes, and geometric coregistration of data from these two sensors. This study investigates a method of using MISR angular observations to supplement available MODIS observations and to improve the quality of the MODIS

Manuscript received October 2, 2001; revised April 3, 2002. This work was supported by NASA's MODIS project under Contract NAS5-31369 and MISR project under Contract NAS7-1407.

Y. Jin, C. B. Schaaf, and A. H. Strahler are with the Department of Geography, Boston University, Boston, MA 02215 USA.

F. Gao and X. Li are with the Department of Geography, Boston University, Boston, MA 02215 USA, and also with the Research Center for Remote Sensing, Beijing Normal University, Beijing, China.

C. J. Bruegge and J. V. Martonchik are with the Jet Propulsion Laboratory, California Institute of Technology, Pasadena, CA 91109 USA.

Publisher Item Identifier 10.1109/TGRS.2002.801145.

TABLE I
MODIS AND MISR SPECTRAL BAND SPECIFICATIONS

	MODIS		MISR	
Band Name	No.	Interval (nm)	No.	Interval (nm)
Blue	3	459 – 479	1	425 – 467
Green	4	545 – 565	2	543 – 572
Red	1	620 – 670	3	661 – 683
NIR	2	841 – 876	4	847 – 886

BRDF/albedo product. The organization of this paper is as follows. We provide a brief description of the instruments and data in Section II. The mathematical formulation of the inverse problem is given in Section III. Section IV examines the additional information content of MISR observations, and Section V presents a preliminary comparison between MODIS and MISR BRFs. A synergistic method is developed in Section VI, which uses the BRDF parameters derived from the MISR observations as *a priori* information. Discussions and summary are given in Sections VII and VIII.

II. INSTRUMENTS AND DATA

MODIS–Terra is a cross-track imager with nearly daily global coverage [25]. Multiple directional samplings are accumulated during each 16-day period [7], [9]. MISR, however, takes a novel approach of imaging the earth almost simultaneously in nine different view directions [26]. Its view angles range from 26.1° to 70.5° in both the forward and aftward directions, as well as nadir looking. The global repeat cycle of MISR is nine days around the equator, and three or four overpasses can be obtained in higher latitudes over a 16-day period. MISR's view angles are arrayed along-track, and hence its observations are almost perpendicular to those of MODIS in the azimuth dimension. Both instruments have similar spectral bands in the visible and near infrared, as shown in Table I. The differences of the band centers are less than 25 nm.

The main data used for our analysis are MODIS cloud-free surface bidirectional reflectances [4] and MISR level 2 BRFs [27]. Both are atmospherically corrected. The MODIS BRF product uses the integerized sinusoidal grid (ISG) projection and has a spatial resolution of 1 km [4], [28], whereas the MISR BRF product uses the space oblique mercator (SOM) projection and has a spatial scale of 1.1 km. The MODIS atmospheric-correction algorithm relies on the simulation of atmospheric effects by 6S radiative transfer code to obtain the surface directional reflectance from the top-of-atmosphere (TOA) reflectance. Both the adjacency effects of environment and the directional effects of surface reflectivity can be considered [4], although at present these corrections have not yet been implemented [28]. In the MISR algorithm, the surface hemispheric directional reflectance factor (HDRF) and the bihemispheric reflectance (BHR) are first retrieved from TOA radiances, and then a parametric BRDF model [29] is used to derive surface bidirectional reflectances [27], [30].

We extracted four ISG tiles of MODIS data acquired from May to October 2001 and chose eight corresponding MISR swath segments to represent different angular sampling patterns and land cover types (Table II). These cases represent the provisional products from the reprocessing of MODIS data and the beta products from the MISR team. The main vegetation types are forests and crop/vegetation mixtures in the northeastern and central U.S. (h12v04 and h10v05). The dominant land cover types are desert and semidesert shrublands in the Sahara region (h18v07) and savannas and shrubs in southern Africa (h20v10). We reprojected the MISR level 2 BRFs and the angular parameters from the space oblique mercator to the integerized sinusoidal grid. The nearest-neighbor technique was then used to resample them to 1-km resolution. By overlaying color composite images of reprojected MISR reflectances on those of MODIS, we find the geometric registration difference is generally within half a pixel. Fig. 1 shows an example tile of the false color images of MODIS surface BRFs acquired on May 26, 2001 and the reprojected MISR surface BRFs acquired by its nadir camera on the same day.

III. FORMULATION OF THE INVERSE PROBLEM

MODIS derives surface BRDF/albedo through the inversion of a semiempirical kernel-driven bidirectional reflectance distribution model [7], [8]. The RossThick–LiSparse–Reciprocal model is a linear combination of two kernels which represent the basic turbid medium scattering $k_{\rm vol}$ and sparse vegetation scattering $k_{\rm geo}$

$$\rho(\lambda;\underline{\Omega}',\underline{\Omega}) = f_{\rm iso}(\lambda) + f_{\rm vol}(\lambda)k_{\rm vol}(\underline{\Omega}',\underline{\Omega}) + f_{\rm geo}(\lambda)k_{\rm geo}(\underline{\Omega}',\underline{\Omega}) \quad (1)$$

where $\underline{\Omega}'$ and $\underline{\Omega}$ denote the illuminating and viewing direction; λ is the wavelength; $f_{\rm iso,vol,geo}$ are BRDF parameters; and $\rho(\lambda;\underline{\Omega}',\underline{\Omega})$ is the surface bidirectional reflectance. Detailed expressions of the above two kernels are listed in [7] and [12].

The inverse problem of the BRDF retrieval with the RTLSR model can be written as the following matrix form:

$$M_{n\times 1} = K_{n\times 3}X_{3\times 1} + E_{n\times 1} \quad (2)$$

where M is the measurement vector in n different viewing and illuminating geometry; K is the kernel matrix; X represents the kernel coefficients to be derived; and E is the measurement noise vector. With a general assumption of random noise with equal expectations of zero, the BRDF parameters can be solved with an ordinary least square method [31] as

$$X_{3\times 1} = \left(K'C_E^{-1}K\right)^{-1}K'C_E^{-1}M \quad (3)$$

where K' is the transpose of the kernel matrix and C_E is the covariance matrix of measurement errors [8]. The covariance of the parameters is

$$C_X = \left(K'C_E^{-1}K\right)^{-1}. \quad (4)$$

In the ideal case of independent errors with equal variances σ^2, the solution can be simplified as

$$X_{3\times 1} = (K'K)^{-1}K'M \quad (5)$$

and its covariance matrix is

$$C_X = (K'K)^{-1}\sigma^2. \quad (6)$$

TABLE II
STUDY AREAS REPRESENTED BY MODIS ISG TILE NUMBER AND MISR PATH/ORBIT AS WELL AS ACQUISITION DATES

		MODIS		MISR	
Lat./Lon.	Dominant LC	Tile No.	Date	Path/Orbit	Date
40°–50°N 93°–65°W	Forests and Mosaic Mixed Forests	h12v04	07/28–08/12 09/14–09/29	P015/O008640 P017/O009310	08/02 09/17
30°–40°N 104°–80°W	Forests and Savannas Cropland and Mosaics	h10v05	05/09–05/24 09/30–10/15	P024/O007461 P021/O009718	05/13 10/15
10°–20°N 0°–10°E	Semi-Desert and Shrublands	h18v07	09/14–09/29	P188/O009277 P192/O009452	09/15 09/27
10°–20°S 22°–33°E	Savannas	h20v10	05/25–06/09	P172/O007645 P176/O007820	05/26 06/07

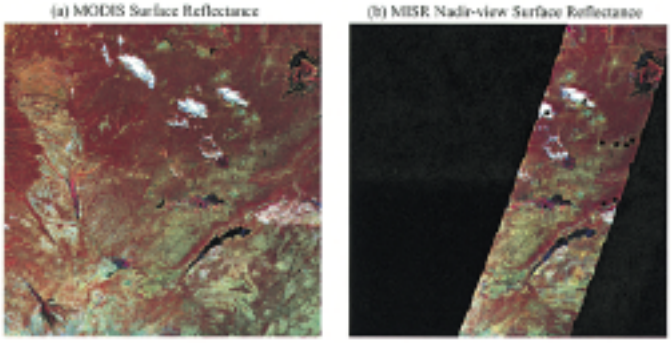

Fig. 1. False color images of surface bidirectional reflectances acquired by MODIS and MISR on May 26, 2001. (a) MODIS BRFs (ISG tile h20v10). (b) MISR nadir-view BRFs (path 172, orbit 7645) reprojected to ISG.

IV. MODIS AND MISR SURFACE DIRECTIONAL REFLECTANCES

A. Angular Signatures

Fig. 2 shows three typical angular sampling patterns of MODIS and MISR under clear sky over the study areas. MODIS samplings cover a similar range of viewing zenith angles, when accumulated over a 16-day period, as those obtained by MISR on a single day. The range of solar zenith angles varies from 10 to 20°. In the azimuth dimension, MODIS and MISR samplings are perpendicular to each other. The observations from both sensors are in between the principal plane (PP) and the cross-principal plane (CPP) over the New England area in August 2001 (Fig. 2, left). MODIS angular samplings are closer to the PP in the Sahelian region in late September 2001 while those of MISR are closer to the CPP (Fig. 2, middle). MISR observations are closer to the PP over southern Africa in May and June 2001 (Fig. 2, right). Cloud obscuration is found to affect the number and the distribution of available MODIS observations, as well as the number of available MISR orbits.

The anisotropy of land surface directional reflectance is a result of the radiative interaction between photons and the soil–vegetation system [10]. The soil–vegetation proportion, vegetation structure, and element optical properties are primary factors governing the angular distribution of the canopy-leaving radiation. Three examples of surface BRFs are displayed in Fig. 3. The angular signatures of surface directional reflectances as observed from MODIS and MISR are very similar in tile h12v04, where both viewing azimuths are between the PP and CPP (Fig. 3, left panel). The backward scattering is obviously stronger than the forward scattering. In tile h20v10 (Fig. 3, right panel), the surface reflectances observed from MISR show larger angular variations than those from MODIS due to the fact that MISR observations are closer to the PP in May/June. The opposite case is observed in tile h18v07 in September (Fig. 3, middle panel). The well-known *hot spot* phenomenon is shown in both the MISR PP case and MODIS PP case. Generally, the MODIS sequentially accumulated observations and the MISR simultaneously acquired multiangle observations capture the primary directional characteristics of vegetation reflectance, such as the stronger backward scattering in all azimuth planes and the hot spot effect in the principal plane.

B. Additional Information Content of MISR Multiangle Observations

The basic rationale for exploring synergistic retrievals is that MISR multiangle observations can bring extra information and constraints to characterize the surface anisotropy and hence albedo. Theoretically, no additional information is added if one data source can be used to perfectly predict the other or if there is no significant difference between surface albedos, as well as their quality assessments individually derived from MODIS or MISR observations. Increasing the number and the diversity of angular samplings should bring additional information, but extra noise from the measurements may also be introduced. These two factors affect the total information gain of introducing additional samplings, as shown by the covariances of retrieved BRDF parameters in (6).

The covariance matrix of BRDF parameters consists of two terms: $(K'K)^{-1}$ merely depends on angular sampling structure, and σ^2 depends on the noise level in measurements. The less the uncertainty, the larger the information. The inverse of the covariance matrix can be taken as a simple measure of the joint information gain of three BRDF parameters through inversion

$$C_X^{-1} = \frac{K'K}{\sigma^2}. \tag{7}$$

Unfortunately, the uncertainty of observations is currently unknown. Assuming the BRDF model is correct, we here approximate the variance of the measurements by the mean square error

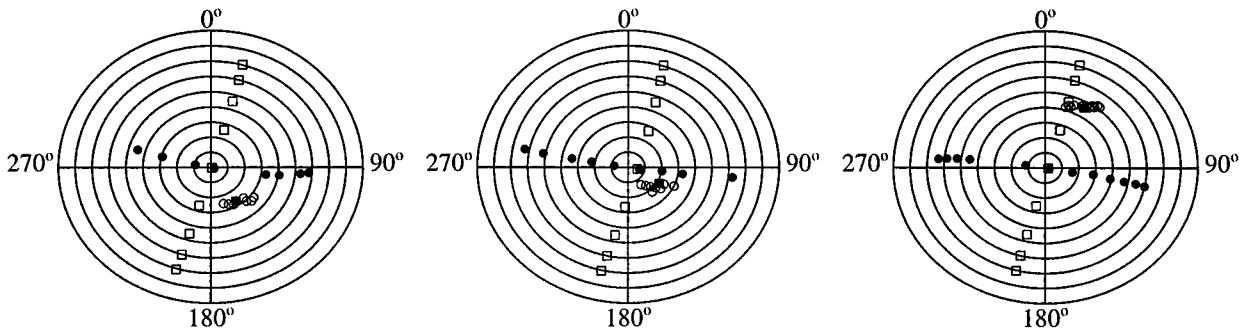

Fig. 2. Angular samplings of MODIS and MISR observations for a pixel in New England in August (left panel, tile h12v04, path 015), a pixel in Sahel in September (middle panel, tile h18v07, path 188), and a pixel in Botswana in May/June (right panel, tile h20v10, path 172). Radius of circles represents zenith angle with 10° increment (zero zenith angle is in the center), and polar angle represents azimuth (zero azimuth, North, is on the top). Solid dot and open square: MODIS and MISR viewing directions; open circle and solid square: sun locations of MODIS and MISR overpass.

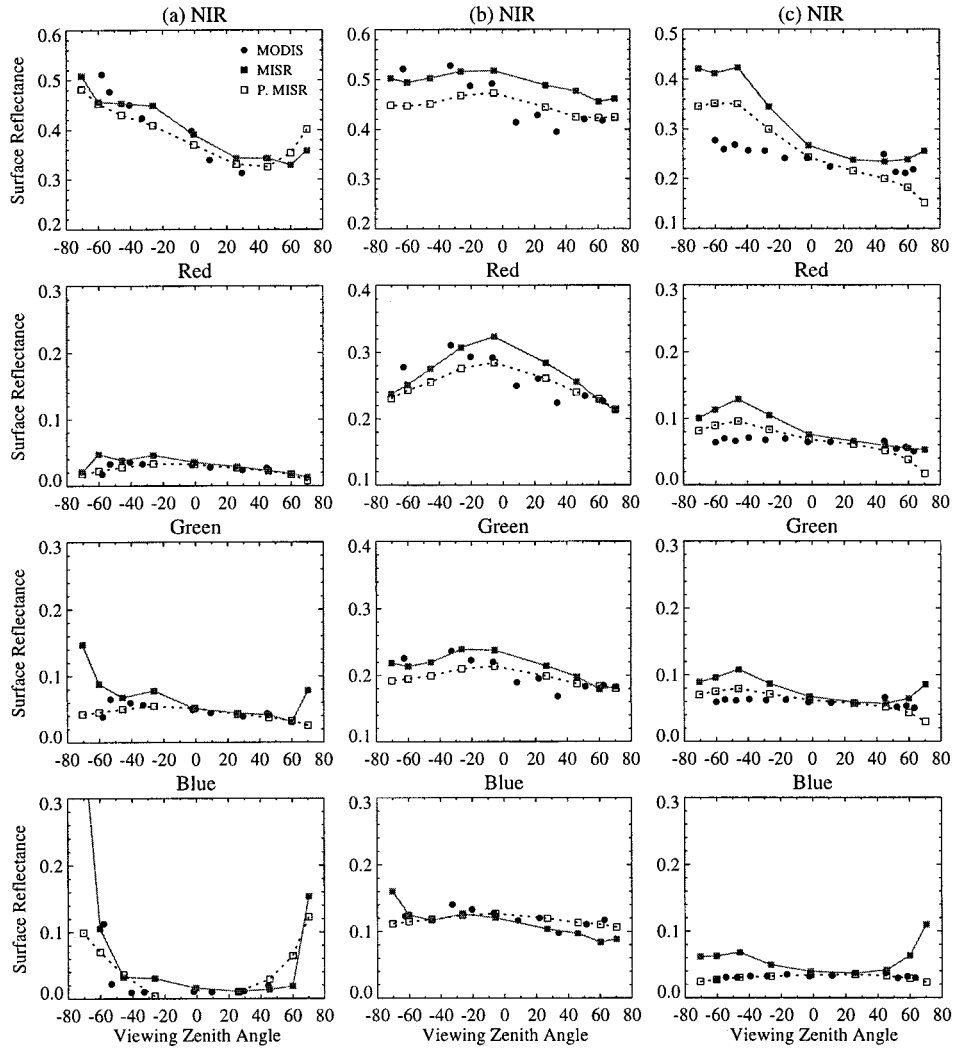

Fig. 3. Surface directional reflectances observed from MODIS (solid dot) and MISR (solid square, solid line) and the predicted surface reflectances at MISR angular geometries (open square, dashed line) using MODIS observations for three pixels shown in Fig. 2. The represented land cover types are broadleaf forest (left panel), sparse shrubs on bare soil (middle panel), and savannas (right panel).

(MSE) between the measurements and the predictions from the inverted RTLSR model. In the above equation, $K'K$ can be decomposed as

$$K'K = G'VG \tag{8}$$

where V is the eigenvalue diagonal matrix, and G is the eigenvectors of $K'K$. According to the widely used Entropy concept in information theory [32], we define an information index I as

$$I = \ln\lambda_1 + \ln\lambda_2 + \ln\lambda_3 - \ln(\mathrm{MSE}) \tag{9}$$

TABLE III
INFORMATION INDEX (MEAN AND STANDARD DEVIATION) FOR VARIOUS MODIS AND MISR SAMPLING SCHEMES AND NET INFORMATION GAIN BY ADDING MISR OBSERVATIONS TO THOSE OF MODIS FOR BRDF/ALBEDO RETRIEVALS

Sampling	I (NIR)	I (Red)	I (Green)	I (Blue)
h20v10, P172 (MISR PP, MODIS CPP)				
MISR only	12.38(0.76)	14.00(0.76)	13.82(1.20)	13.32(1.20)
MODIS only	7.91(1.69)	8.94(2.11)	9.28(2.25)	9.50(2.39)
MODIS+MISR	11.79(1.13)	13.40(1.64)	13.41(1.57)	12.92(1.42)
Net Info. Gain	3.88(1.50)	4.46(1.36)	4.14(1.55)	3.42(1.89)
h12v04, P015 (both between CPP and PP)				
MISR only	8.50(1.64)	10.73(1.64)	9.35(1.93)	7.63(2.06)
MODIS only	6.61(1.09)	9.17(2.31)	9.12(2.13)	9.08(2.41)
MODIS+MISR	8.56(2.07)	11.29(2.62)	10.53(1.89)	9.13(1.95)
Net Info. Gain	1.95(2.32)	2.12(2.67)	1.40(2.45)	0.05(2.90)
h18v07, P188 (MISR CPP, MODIS PP)				
MISR only	6.62(1.02)	7.09(1.02)	6.44(1.19)	6.97(1.40)
MODIS only	8.91(0.98)	9.51(0.90)	10.22(0.93)	10.54(0.92)
MODIS+MISR	8.03(1.33)	9.34(0.94)	9.54(0.96)	8.94(0.80)
Net Info. Gain	-0.88(1.55)	-0.18(1.14)	-0.68(1.13)	-1.59(1.05)

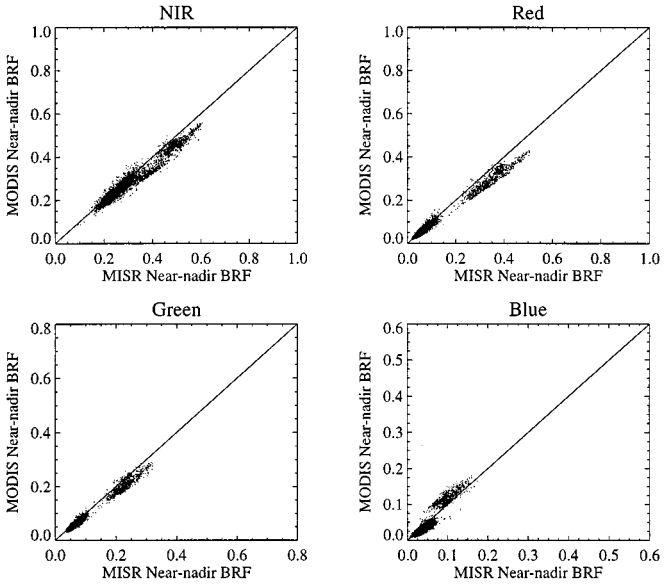

Fig. 4. Scatter plots of MODIS- versus MISR-observed near-nadir surface reflectances over eight swath segments listed in Table II in the near infrared, red, green, and blue. The solid line is 1:1 line. Note that no spectral adjustment was performed for the intercomparison analysis.

where $\lambda_{1,2,3}$ are diagonal elements of the matrix V. Based on the information index (I), the net information gain $I_{\rm net}$ of adding MISR observations to the retrieval with MODIS-only observations is defined as

$$I_{\rm net} = I^{\rm MODIS+MISR} - I^{\rm MODIS}. \tag{10}$$

It is the balance of the information gain from additional samples and the information loss from extra noise.

Paths 015, 188, and 172 represent the three typical sampling patterns, as shown in Fig. 2. We calculated the information index of MISR-only observations, MODIS-only observations, and MODIS plus MISR observations, respectively, and then derive the net information gain for each pixel in these three swath segments. Table III shows the mean values and standard deviations of the information index when MODIS has more than six angular samples. When MISR sampling is closer to the principal plane than that of MODIS (path 172), the combined sampling is shown to bring net information gain to MODIS-only observations. The net information gain from MISR sampling is increased when the number of MODIS observations closer to CPP is further reduced. The net information gain is less significant when both MODIS and MISR observations are between PP and CPP (path 015). Generally, adding MISR CPP sampling to MODIS PP observations (path 188) does not result in a net information gain due to the smaller information/noise ratio in the CPP, except for a small number of cases when MODIS acquires less than three clear-sky observations. Table III also shows that the net information gain also depends on the wavelength and that the information gain is higher in the red and near infrared than in the green and blue.

V. SYNERGISM BETWEEN MODIS AND MISR SURFACE DIRECTIONAL REFLECTANCES

Theoretically, MODIS and MISR should produce comparable surface BRF products after accounting for possible spectral differences and could be combined directly for a synergistic retrieval. The actual surface BRF products, however, are affected by both TOA inputs and prerequisite aerosol retrieval. The significant difference between MODIS and MISR angular sampling geometries (Fig. 2) further makes the comparison of surface bidirectional reflectances derived from these two instruments a challenge. To compare the off-nadir directional reflectances, a BRDF model must be inverted with the observations from individual instruments, and then the derived parameters can be used to predict reflectances at common view angles. This method potentially includes any uncertainty issues confronted by the BRDF model and its inversion, as well as the reflectance prediction. It complicates our goal of investigating the compatibility of the actual MODIS and MISR BRF products. However, we observe the possibility that the similar angular samplings appear close to the nadir, where a direct comparison can be made.

A. Surface BRFs

To ensure the similarity of sun–view geometry, we extracted near-nadir observations (both viewing zenith angles and the relative azimuth difference less than 5°) acquired on the same day from MODIS and MISR. The scatter plots of MODIS BRFs versus MISR BRFs at near-nadir show that almost all pixels are located along a 1:1 line (Fig. 4). Two clusters are apparent, since desert and semidesert have much higher visible reflectances than vegetated land surface.

The relative difference is calculated as $\left(\rho^{\rm MODIS} - \rho^{\rm MISR}\right) / \rho^{\rm MISR}$. Fig. 5 indicates a nearly normal distribution of the relative differences between the MODIS and MISR BRFs in the near infrared, red, and green. The distribution is relatively flatter in the blue. Table IV summarizes the mean values and standard deviations for each swath segment. It shows that the mean relative difference depends more or less on the specific swath, especially for the blue band. In the near infrared, the mean relative

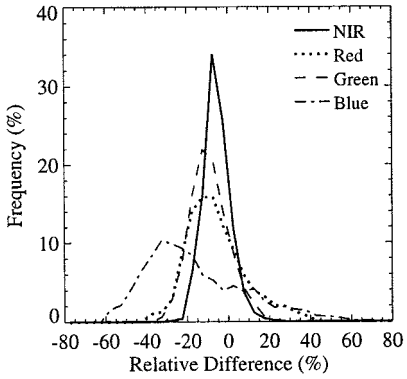

Fig. 5. Distributions of relative differences between MISR and MODIS near-nadir surface reflectances in the near infrared (solid), red (dotted), green (dashed), and blue (dashed-dotted) over study areas.

difference ranges from −1.5 to −7.1% among various swath segments of the vegetated land areas (the first five swath segments in Table IV), and its standard deviations are less than 7%. In the red, the relative difference is more variable. The MODIS reflectance is higher than that of MISR by 7% in the red in tile h12v04, but lower than that of MISR by around 5% for other vegetated areas. The largest differences are found in the blue band, particularly where the MODIS BRFs are higher in desert/semidesert tile h18v07 but lower in other vegetated tiles. The relative difference in the green is roughly between those in the red and blue. The variation of relative differences is generally less than 10% in the near infrared and green and higher in the red and blue.

Surface BRF products depend on atmospheric corrections. Aerosol retrieval plays a critical role, since aerosol scattering has a large impact on the visible and near infrared signals. MISR aerosol products at 17.6-km resolution [30] are used in the processing of its surface radiative properties. MODIS level 2 aerosol product at 10-km resolution, however, is not directly used in the MODIS atmospheric correction scheme. A new version of the aerosol algorithm was developed specifically for the MODIS surface reflectance algorithm to extend the aerosol retrieval to brighter targets and obtain retrievals at a much higher spatial resolution (1 km) [28]. Unfortunately, this updated intermediate 1-km aerosol product is not currently output as a product and not available to us. Therefore, a quantified analysis of the contribution of aerosol retrieval and atmospheric correction to surface BRF differences cannot be undertaken in this study.

B. Top-of-Atmosphere BRFs

Surface BRFs are derived from the TOA reflectance through atmospheric correction. A comparison of the MODIS and MISR TOA near-nadir directional reflectance factor is essential for understanding the effect of instrument calibration, spectral specification, and georegistration on the surface BRF products. *Bruegge et al.* [24] found that the effect of MODIS and MISR spectral response differences on TOA radiances was significant in the blue. The TOA radiance scale factor—the ratio of the integral of the TOA upwelling spectral radiance convoluted with MISR spectral response functions over that with MODIS spectral response functions—was also shown to depend on surface type, such as 0.906 for Lunar Lake desert scenes and 1.054 for ocean scenes in the blue [24]. Validation of MISR TOA radiance [24] over the calibration sites demonstrated that the MISR and MODIS TOA radiance products agree within an uncertainty of 3% after a spectral adjustment, indicating a good agreement between the calibrations of both instruments.

We examine here the overall comparability between MODIS and MISR TOA nadir reflectances over our study areas. For those pixels extracted for the near-nadir surface BRF comparison, we calculated MODIS and MISR TOA BRFs from a MODIS-aggregated 1-km TOA radiance product (MOD021KM) and a MISR L1B2 nadir-camera radiance product with 275-m resolution, respectively. The reflectance scale factor and offset contained in MOD021KM metadata are directly applied to convert MODIS radiance to reflectance. MISR TOA reflectance is calculated with

$$\rho^{\mathrm{TOA}}(\lambda;\theta',\theta_0)=\frac{L(\lambda;\theta',\theta_0)\pi d^2}{E_0(\lambda)\times\cos(\theta_0)} \tag{11}$$

where $L(\lambda;\theta',\theta_0)$ is the TOA radiance; d is the earth–sun distance in astronomical units (AU) contained in the MISR geometric product; and E_0 is the exoatmospheric irradiance which is contained in the MISR ancillary radiometric product [33].

Table IV shows that the agreement of the MODIS and MISR TOA BRFs are better than that of the surface BRFs. There is no significant bias in the TOA BRFs observed by the two instruments, with the mean relative differences mostly less than 6% in the near infrared, red, and green. The difference of variation is also very small. Note that no spectral adjustment was attempted, and therefore our results here include all possible noise from spectral differences, geometric coregistration, and spatial aggregation. In the blue band, MODIS TOA BRFs are systematically lower than that of MISR by 7% in the desert and by 16% in the vegetated land, which is possibly due to the different spectral response functions of the two instruments.

The residual of surface BRF differences from TOA BRF differences most likely indicates the effect of different atmospheric corrections on surface BRF differences. Table IV shows that the additional systematic differences introduced by atmospheric correction are generally less than 5% for the vegetated land, except in the blue where the reflectance signal is very sensitive to aerosol scattering. In the desert area, atmospheric correction has a larger effect.

C. Implication for Data Fusion

Ideally, observations from MODIS and MISR can be directly combined together for BRDF and albedo retrievals, hereafter referred as direct synergism, if there is no systematic bias between two datasets or if validated radiometric adjustment coefficients are available. The analysis from the above case studies shows that the MODIS surface near-nadir BRFs generally agree well with those of MISR except in the blue, but atmospheric correction may bring systematic differences, depending on the aerosol retrievals. For a direct synergism with original or adjusted MODIS and MISR BRFs, it is necessary to perform detailed accuracy assessments and uncertainty analyses of both MODIS and MISR surface BRF products. Various efforts are underway to analyze the TOA radiometric difference due to MODIS and MISR spectral specifications [24] and to validate

TABLE IV
RELATIVE DIFFERENCES (MEAN AND STANDARD DEVIATION) BETWEEN MODIS AND MISR SURFACE (AND TOA) NEAR-NADIR BRFS IN PERCENTAGE. NOTE THAT NO SPECTRAL ADJUSTMENT WAS PERFORMED. NO TOA COMPARISON WAS MADE OVER P176 AND P192 DUE TO DATA LIMITATIONS

	Surface Nadir BRFs				TOA Nadir BRFs			
Path	NIR	Red	Green	Blue	NIR	Red	Green	Blue
P015	-0.2(8.9)	6.6(17.0)	1.6(9.6)	-14.0(21.2)	-5.2(4.0)	-0.1(6.8)	-3.9(3.0)	-17.1(1.6)
P017	-7.1(6.2)	9.6(14.7)	-5.1(6.0)	-27.7(10.1)	-3.4(5.7)	2.6(7.7)	-3.8(2.9)	-17.6(1.9)
P021	-5.3(6.0)	-3.7(12.8)	-8.0(7.8)	-26.4(10.4)	-4.6(4.8)	-1.8(7.0)	-2.9(4.2)	-16.9(2.4)
P172	-8.0(7.0)	-5.5(11.5)	-9.8(7.4)	-20.9(16.7)	-5.8(3.9)	-3.5(6.4)	-6.2(3.1)	-16.3(2.1)
P176	-4.7(6.1)	-6.8(10.3)	-11.2(8.5)	-20.8(15.1)				
P188	-10.2(5.7)	-18.0(5.6)	-13.3(5.4)	15.7(12.1)	-6.0(3.3)	-9.3(4.8)	-4.8(3.5)	-6.9(2.7)
P192	-7.1(5.1)	-11.1(5.0)	-4.2(6.1)	20.1(15.0)				

MODIS and MISR surface BRFs and characterize their accuracy [28], [34]. Further study of direct synergism can be undertaken after these evaluation and validation efforts are completed. In Section VI, we explore an *a priori* synergistic approach to combine the observations from the two instruments in a flexible way. Given the large differences exhibited in the blue, the synergism in the blue will not be included in Section VI.

VI. *A PRIORI* SYNERGISM

A. Using A Priori Knowledge

One major concern in combining multisource data is the possibility of introducing more noise than new information. As one of the major land products of MODIS, consistency is a critical issue when attempting to add information from MISR observations to improve MODIS BRDF/albedo retrievals. Our objective is to incorporate the directional information of MISR BRFs and at the same time to minimize the effect of any possible systematic discrepancy in magnitude due to spectral specification, geometric coregistration, and atmospheric correction.

The anisotropic shape information is contained in the BRDF parameters. The unique property of the simultaneous multiangle observations of MISR guarantees that we either get a sufficient number of looks covering both forward and backward directions under clear sky or obtain nothing at all due to clouds. Therefore, when MISR observations are available and MODIS sampling is poor, we can use the BRDF parameters derived from the original MISR observations as *a priori* knowledge and couple these with the available MODIS observations during a 16-day period to get *a posteriori* estimates of the BRDF parameters. The cost function is written as

$$\mathrm{Cost}(X) = (KX - M)'(KX - M) + \gamma(X - X_{\mathrm{priori}})'(X - X_{\mathrm{priori}}) \quad (12)$$

where X_{priori} is the *a priori* parameter vector derived from MISR observations, and γ is the weight with which *a priori* information is incorporated [17], [19]. The first term is the cost of data misfit and the second term the deviation from an *a priori* guess. In this way, the retrieval is a balance of the data fitting and *a priori* information. The solution is given by [19]

$$X = (K'K + \gamma U)^{-1}(K'M + \gamma X_{\mathrm{priori}}) \quad (13)$$

where U is a 3-by-3 unit matrix.

B. Sensitivity Analysis

The question arises as how to select an appropriate weight γ. Conceptually, it depends on the information content in the MISR sampling and the noise level in the MISR surface BRF product relative to those of the MODIS product. We first examine how *a priori* synergistic retrieval performs with values of γ. Using the data from our case studies, we derived corresponding albedos and predicted surface reflectances by changing the relative weight, according to (13). We took the retrieval from a direct synergism with the MODIS and MISR BRFs adjusted by the nadir BRF as a reference. Note that for the sensitivity analysis here we emphasize the trend of retrieval errors with γ instead of the absolute values of actual errors. The relative retrieval errors in white sky albedo and surface BRFs under MODIS and MISR sun–view geometries are plotted against the value of γ in Fig. 6 (solid line) for the pixel shown in the right panel of Fig. 3. To investigate the effect of variable MODIS sampling, we also subsetted the MODIS observations to represent the cases that MODIS samplings cover backward only (dotted line), backward plus one near-nadir forward (dashed line), and backward plus one far-off-nadir forward (dash dot line) scattering.

The relative retrieval errors of BRFs decrease rapidly as the weight of the *a priori* information increases, especially in the cases where the MODIS samples are mainly distributed in the backward direction. This indicates that the injection of *a priori* knowledge can improve the retrieval accuracy even with a small weight. The retrieval errors of both albedo and BRFs for various MODIS sampling schemes become stable with an increase of the weight and converge when the weight is around 5.0. For comparison, Fig. 6 also plots the results from the direct synergism with the original MISR observations and four types of MODIS samplings as symbols over the $\gamma = 0$ line. Clearly, the direct synergism results in much larger relative errors of albedo retrievals than *a priori* synergism.

In an attempt to investigate the effect of any possible systematic differences between the MODIS and MISR BRFs on *a priori* synergism, we intentionally changed the magnitude of the MISR BRFs in our case study while keeping the reference unchanged, and we found that the sensitivity to the weight stays the same. When MISR BRFs are increased by 10% as a severe test (see Fig. 7), the relative error of BRF prediction increases from 9 to 13% in the red and from 6 to 9% in the near infrared.

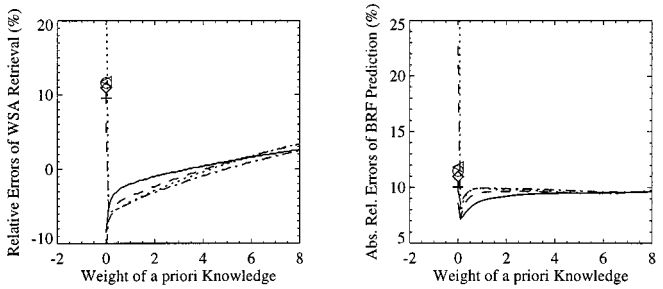

Fig. 6. Sensitivity of relative retrieval errors for white sky albedo (left panel) and BRF retrievals (right panels) in the red to the weight of *a priori* knowledge of BRDF parameters derived from MISR observations close to the principal plane. MODIS samplings used for the *a priori* synergism scheme are: all (solid line), backward (dotted line), backward plus one near-nadir forward (dashed line), and backward plus one far-off-nadir forward (dashed-dotted line). Results from the direct synergism approach with the original MODIS and MISR observations are plotted with plus, open triangle, open circle, and open diamond for the above MODIS samplings, respectively.

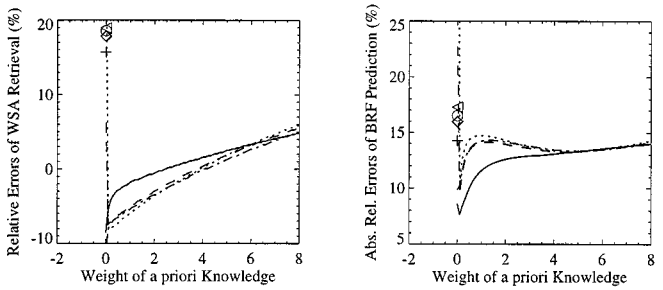

Fig. 7. Same as Fig. 6, but the MISR BRFs used to derive the *a priori* knowledge are intentionally increased by 10%.

The relative errors of white sky albedo are very stable. Compared to *a priori* synergism, the direct synergistic method, however, is more sensitive to the magnitude shift of *a priori* observations and has much lower retrieval accuracies, especially for white sky albedo retrieval (Fig. 7). This implies that the *a priori* synergism is a better choice than direct synergism in the case when a systematic bias between MODIS and MISR BRFs may be present or is uncertain.

When MISR observations are close to the cross-principal plane and those of MODIS are close to the principal plane (the pixel shown in the middle panel of Fig. 3), the relative retrieval errors of albedo and BRFs from *a priori* synergism reach the minimum when the weight is between 0.1 and 0.3 and then increase with the weight. This low value of relative weight is probably due to the reduced information contained in the CPP observations. Moreover, the retrieval in this case is more dependent on the sampling geometry of MODIS. In particular, relative retrieval errors are smaller if the MODIS PP samplings include both the forward and backward directions and are less sensitive to the weight of *a priori* knowledge.

C. Weight of A Priori Knowledge

The information index as shown in Section IV captures the information content from a particular sampling through inversion. We rely on the net information gain $I_{\rm net}$ as a criterion as to whether to include MISR observations or not. When there is net information gain, adding MISR observations brings more information than noise to MODIS BRDF/albedo retrievals. The larger the information content of MISR observations relative to those of MODIS, the larger the weight γ of *a priori* knowledge from MISR should be taken in a synergistic retrieval. Here, we take the ratio of the information index for MISR observations over that for MODIS observations as an approximation for the weight of *a priori* knowledge. In path 172, the mean value of the information ratio is 1.65, 1.68, and 1.60, respectively, for the near infrared, red, and green. Note that these values are in the range of γ values where retrieval is relatively insensitive to γ compared to the most sensitive region when γ is less than 1.0.

To examine how this method performs, we use the PARABOLA BRF measurements of old jack pine over boreal forests [35] as an example, due to the current lack of analyzed ground-based validation information associated with MODIS and MISR observations. We extracted measurements with the angular sampling patterns similar to those of the MODIS CPP and MISR PP case. The white sky albedo from the retrieval with all observations is 0.0328 in the red. The retrieval with the PP measurements alone is 0.0358, and the retrieval with the CPP measurements alone is 0.0177. When using BRDF parameters from the PP measurements as *a priori*, the information ratio is 1.81, and the white sky albedo retrieved through *a priori* synergism is 0.0333, which is very close to the true value. The improvement is less obvious in the near infrared where only slight improvement is found. When we add a bias of 10% to the PP measurements, the white sky albedo from *a priori* synergism is only increased to 0.0337. However, the white sky albedo from a direct synergism is rapidly increased to 0.0362.

D. Results From A Priori Synergism Applied to MODIS and MISR Case Studies

Using the BRDF parameters derived from the original MISR BRFs as *a priori*, we injected the MODIS observations and obtained new BRDF parameters. As an example, Fig. 8 presents the predicted BRFs at MODIS and MISR sun–view geometries through *a priori* synergistic retrieval for the pixel shown in the right panel of Fig. 3. It is clear that the derived BRDF can capture the shape of angular reflectances of both MODIS and MISR, and the magnitude is between the MODIS- and MISR-observed reflectances. Generally, the predicted BRFs at the MISR angular geometries are lower than the MISR BRFs, and the predicted BRFs at MODIS geometries are very similar to the MODIS BRFs. It should also be noted that the near-nadir reflectances are better preserved than the off-nadir reflectances.

For the May–June case in tile h20v10, the MISR observations are closer to the principal plane and were shown to bring significant net information gain (Section IV). We did three sets of inversions with the MISR-only observations, MODIS-only observations, and the *a priori* retrieval. The correlation between the MISR-observed BRFs and those predicted through inversion of MODIS observations for each pixel was chosen as a measure of the similarity between the observed and predicted BRDF shapes, since it is not affected by any systematic magnitude differences between two products. On the average, the correlation coefficient between the observed and predicted MISR surface BRFs increases from 0.89 to 0.97 in the near infrared, 0.65 to 0.94 in the red, 0.47 to 0.89 in the green, when using *a priori* synergism, compared to using the MODIS-only observations for retrieval. For surface BRFs at the MODIS sampling ge-

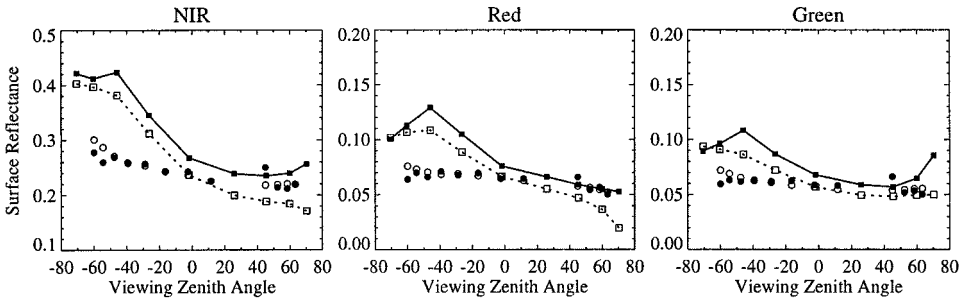

Fig. 8. Surface directional reflectances at MODIS (open circle) and MISR (open square, dashed line) sampling geometries derived from *a priori* synergism with the original MODIS and MISR surface reflectances for the pixel shown in the right panel of Fig. 3. The MODIS BRFs (solid circle) and MISR BRFs (solid square, solid line) are also plotted for comparison. The relative weight used for *a priori* knowledge is 1.7, calculated as the ratio of MISR information index over MODIS information index.

TABLE V
MEAN RELATIVE PREDICTION ERRORS (PERCENT) IN THE NEAR INFRARED, RED, AND GREEN FOR RETRIEVALS WITH MODIS OBSERVATIONS ALONE, MISR OBSERVATIONS ALONE, AND *A PRIORI* SYNERGISM OVER ISG TILE H20V10 (PATH 172 AND 176). IGBP LAND COVER TYPES: 2. EVERGREEN BROADLEAF FOREST; 8. WOODY SAVANNAS; 9. SAVANNAS; 10. GRASSLANDS; 12. CROPLANDS

Predict	MISR		MODIS		MODIS+MISR		
			using				
LC	MODIS	*a priori*	MISR	*a priori*	MISR	MODIS	*a priori*
			Near Infrared Band				
2	13.6	9.6	12.1	4.5	8.0	8.0	6.9
8	13.8	10.2	13.1	4.3	8.6	7.9	7.0
9	15.5	12.2	16.6	4.9	10.0	9.5	8.3
10	15.6	13.0	18.3	5.8	10.6	10.4	9.3
12	15.3	11.9	17.1	5.7	10.1	10.2	8.7
All	14.9	11.2	8.3	5.1	9.4	9.2	7.9
			Red Band				
2	24.4	16.9	20.2	6.1	12.8	13.5	11.1
8	28.4	16.9	19.4	7.3	13.1	15.9	11.7
9	38.9	19.4	23.1	11.7	15.1	23.7	15.2
10	30.8	15.1	20.8	13.6	12.9	21.7	14.4
12	32.8	16.7	22.5	13.8	14.3	22.7	15.3
All	35.4	18.7	21.7	10.6	14.1	21.5	14.3
			Green Band				
2	20.6	14.1	18.3	5.8	11.7	11.5	9.7
8	22.8	14.7	20.1	7.0	13.5	12.9	10.5
9	38.9	19.4	23.1	11.7	15.1	23.7	15.2
10	28.7	15.9	24.8	14.0	15.2	20.5	14.9
12	27.6	16.1	25.4	13.4	16.1	19.8	14.7
All	27.7	16.1	22.3	10.2	14.4	17.4	12.9

ometries, the correlation coefficient between observations and the prediction in this case only decreases slightly by 0.1 in the red and green. Overall, this indicates that *a priori* synergism can improve the representation of the surface BRDF shape in comparison with the inversion from the MODIS CPP observations alone.

For various land cover types, the relative prediction errors through different retrievals are summarized in Table V for the red, green, and near infrared for the May–June case. In the red band, the error of predicting all combined MODIS and MISR observations is reduced to 14.3% with *a priori* synergism, compared to 21.5% with the inversion from MODIS-only CPP observations, but is similar to that of using MISR-only BRFs acquired close to the PP. The *a priori* synergistic retrieval predicts MODIS BRFs with the mean relative error of 10.6% and MISR BRFs with 18.7%. However, the mean relative error is as high as 21.7% for the prediction of the MODIS BRFs with the MISR PP observations alone and 35.4% for the prediction of the MISR BRFs with the MODIS CPP observations alone, respectively. Similar results are found for the green band. The prediction of MODIS BRFs with *a priori* synergism has lower errors than the prediction of MISR BRFs, indicating that the magnitude of the MODIS surface BRFs is better preserved. This is a great benefit for the consistency of MODIS products. Table V also demonstrates that the accuracy improvement is more significant for savannas, grasslands, and croplands than for broadleaf forests and woody savannas. The improvement in the near infrared is not so significant.

The above analysis indicates that the total inversion error is basically determined by the overall information content and noise level in the individual or combined observations. The retrievals with data from individual instruments tend to minimize the error of the BRF prediction over their own sampling schemes, but the prediction error at the angular geometries of the other instrument is higher. On the contrary, the synergistic retrieval takes into account the angular signatures of both observations, and the BRDF is hence better constrained.

VII. DISCUSSION

The inverted BRDF model from a finite set of observations provides a practical and efficient way to characterize the anisotropy of surface reflectivity. An issue confronting the accuracy and hence the application of the BRDF inversion is the sparse or not well-distributed directional sampling available from an individual satellite [13]. MODIS BRDF/albedo retrieval uses the *"sequential"* multiangle concept to obtain directional information from space, while the MISR instrument and its land products use the *"simultaneous"* observation concept [36]. In the growing and senescent seasons, the surface radiative property changes, which may cause a higher noise in the sequential observations than in the simultaneous observations. The choice of time period is a trade-off between the stability of surface reflectivity and the ability to obtain sufficient angular samples due to cloud cover.

During a 16-day period, the number and distribution of MODIS viewing zenith angles are variable due to cloudiness. MISR directional samplings, however, are symmetric in the viewing hemisphere, and only the azimuth component changes significantly with the latitude and season. The MISR observations usually cover a smaller range of solar zenith angles than those of MODIS during a 16-day period though. In the azimuth dimension, MODIS and MISR observations are almost perpendicular to each other. This study takes advantage of such complementary samplings to improve the MODIS BRDF and albedo retrieval. The MISR PP case was shown to bring significant net information gain to MODIS CPP observations and was further explored with *a priori* synergism. The net information gain decreases as MISR observations are far from the principal plane. In particular, the net information gain is negative in the MISR CPP case, and thus *a priori* synergism was not performed.

Compatibility is crucial in utilizing multisource data. Surface BRF is a high-level product, and any uncertainties associated with the TOA reflectance and the prerequisite aerosol retrieval will be transferred down through the processing stream. The intercomparison of surface BRF products from different instruments thus becomes a very complicated task. Contemporary observations from space instruments and *in situ* field measurements are of vital importance to validate the retrieved surface BRFs and to quantify the contributions of various sources to any surface BRF differences. Cooperative validation efforts are currently underway within the EOS instrument, atmosphere, surface, and validation teams, and further refinements to the surface products can be expected as a result of these validation studies. Note that MODIS completed reprocessing a consistent one-year product in January 2002 and that the MISR surface retrievals will be further improved in early 2002 [37]. Thus, the comparison case studies shown in this paper are preliminary and meant to capture the compatibility of these particular datasets.

VIII. Summary

Both MODIS-accumulated and MISR simultaneously obtained observations are found able to capture the primary characteristics of surface anisotropic reflectance. Our preliminary case studies show that MODIS and MISR near-nadir surface BRFs are generally comparable in the near infrared, red, and green. Also shown is that MISR observations bring extra information to the MODIS BRDF/albedo retrievals, especially when MISR acquires observations closer to the principal plane. By taking the BRDF parameters derived from the original MISR observations as *a priori* information, *a priori* synergism appears to improve the representation of the surface BRDF shape and the surface BRDF/albedo retrieval particularly by 10% in the red and green band. Future efforts will be devoted to work with MODIS BRDF/albedo validation scientists to evaluate the *a priori* synergistic method.

Acknowledgment

The authors thank D. Diner and two anonymous reviewers for their valuable comments. MISR data were obtained from the NASA Langley Research Center Atmospheric Sciences Data Center.

References

[1] *Geometrical Considerations and Nomenclature for Reflectance*, NBS Monogr. 160, 1977.

[2] J. V. Martonchik, C. J. Bruegge, and A. H. Strahler, "A review of reflectance nomenclature used in remote sensing," *Remote Sens. Rev.*, vol. 19, pp. 9–20, 2000.

[3] M. Leroy and O. Hautecoeur, "Anisotropy-corrected vegetation indexes derived from POLDER/ADEOS," *IEEE Trans. Geosci. Remote Sensing*, vol. 37, pp. 1698–1708, May 1999.

[4] E. F. Vermote, N. Z. El Saleous, C. O. Justice, Y. J. Kaufman, J. L. Privette, L. Remer, J. C. Roger, and D. Tarne, "Atmospheric correction of visible to middle infrared EOS-MODIS data over land surface, background, operational algorithm and validation," *J. Geophys. Res.*, vol. 102, pp. 17131–17141, 1997.

[5] J.-L. Roujean, D. Tanre, F.-M. Breon, and J.-L. Deuze, "Retrieval of land surface parameters from airborne POLDER and bidirectional reflectance distribution function during HAPEX-Sahel," *J. Geophys. Res.*, vol. 102, pp. 11201–11218, 1997.

[6] G. P. Asner, "Contributions of multi-view angle remote sensing to land-surface and biogeochemical research," *Remote Sens. Rev.*, vol. 18, pp. 137–162, 2000.

[7] W. Lucht, C. B. Schaaf, and A. H. Strahler, "An algorithm for the retrieval of albedo from space using semiempirical BRDF models," *IEEE Trans. Geosci. Remote Sensing*, vol. 38, pp. 977–998, Mar. 2000.

[8] A. H. Strahler, W. Wanner, C. B. Schaaf, X. Li, B. Hu, J.-P. Muller, P. Lewis, and M. J. Barnsley, "MODIS BRDF/albedo product: Algorithm theoretical basis document," NASA EOS-MODIS Doc., Ver. 4.0, 1996.

[9] C. B. Schaaf, F. Gao, A. H. Strahler, W. Lucht, X. Li, T. Tsang, N. C. Strugnell, X. Zhang, Y. Jin, J.-P. Muller, P. Lewis, M. Barnsley, P. Hobson, M. Disney, G. Roberts, M. Dunderdale, C. Doll, R. d'Entremont, B. Hu, S. Liang, and J. L. Privette, "First operational BRDF, albedo and nadir reflectance products from MODIS," *Remote Sens. Environ.*, to be published.

[10] R. B. Myneni, G. Asrar, and F. G. Hall, "A three-dimensional radiative transfer model for optical remote sensing of vegetated land surfaces," *Remote Sens. Environ.*, vol. 41, pp. 85–103, 1992.

[11] X. Li and A. H. Strahler, "Geometric-optical bidirectional reflectance modeling of the discrete crown vegetation canopy: Effect of crown shape and mutual shadowing," *IEEE Trans. Geosci. Remote Sensing*, vol. 30, pp. 276–292, Mar. 1992.

[12] W. Wanner, X. Li, and A. H. Strahler, "On the derivation of kernels for kernel-driven models of bidirectional reflectance," *J. Geophys. Res.*, vol. 100, pp. 21077–21089, 1995.

[13] J. L. Privette, T. F. Eck, and D. W. Deering, "Estimating spectral albedo and nadir reflectance through inversion of simple BRDF models with AVHRR/MODIS-like data," *J. Geophys. Res.*, vol. 102, pp. 29529–29542, 1997.

[14] B. Hu, W. Lucht, X. Li, and A. H. Strahler, "Validation of kernel-driven models for global modeling of bidirectional reflectance," *Remote Sens. Environ.*, vol. 62, pp. 201–214, 1997.

[15] P. Bicheron and M. Leroy, "Bidirectional reflectance distribution function signatures of major biomes observed from space," *J. Geophys. Res.*, vol. 105, pp. 26669–26681, 2000.

[16] W. Lucht and J.-L. Roujean, "Considerations in the parametric modeling of BRDF and albedo from multiangular satellite sensor observations," *Remote Sens. Rev.*, vol. 18, pp. 343–379, 2000.

[17] X. Li, F. Gao, J. Wang, and A. Strahler, "A priori knowledge accumulation and its application to linear BRDF model inversion," *J. Geophys. Res.*, vol. 106, pp. 11925–11935, 2001.

[18] W. Lucht, "Expected retrieval accuracies of bidirectional reflectance and albedo from EOS-MODIS and MISR angular sampling," *J. Geophys. Res.*, vol. 103, pp. 8763–8778, 1998.

[19] S. Twomey, *Introduction to the Mathematics of Inversion in Remote Sensing and Indirect Measurement*. New York: Dover, 1977.

[20] C. D. Rodgers, *Inverse Methods for Atmospheric Sounding: Theory and Practice*. London, U.K.: World Scientific, 2000.

[21] M. J. Barnsley, A. H. Strahler, K. P. Morris, and J.-P. Muller, "Sampling the surface bidirectional reflectance distribution (BRDF): 1. Evaluation of current and future satellite sensors," *Remote Sens. Rev.*, vol. 8, pp. 271–311, 1994.

[22] W. Lucht and P. Lewis, "Theoretical noise sensitivity of BRDF and albedo retrieval from the EOS-MODIS and MISR sensors with respect to angular sampling," *Int. J. Remote Sens.*, vol. 21, pp. 81–98, 2000.

[23] W. L. Barnes, T. S. Pagano, and V. V. Salomonson, "Prelaunch characteristics of the Moderate Resolution Imaging Spectroradiometer (MODIS) on EOS-AM1," *IEEE Trans. Geosci. Remote Sensing*, vol. 36, pp. 1088–1100, July 1998.

[24] C. J. Bruegge, N. L. Chrien, R. R. Ando, D. J. Diner, W. A. Abdou, M. C. Helmlinger, S. H. Pilorz, and K. Thome, "Early validation of Multi-angle Imaging SpectroRadiometer (MISR) radiometric data products," *IEEE Trans. Geosci. Remote Sensing*, vol. 40, pp. 1477–1492, July 2002.

[25] C. O. Justice, E. Vermote, J. R. G. Townshend, R. Defries, D. P. Roy, D. K. Hall, V. V. Salomonson, J. L. Privette, G. Riggs, A. Strahler, W. Lucht, R. B. Myneni, Y. Knyazikhin, S. W. Running, R. R. Nemani, Z. Wan, A. R. Huete, W. v. Leeuwen, R. E. Wolfe, L. Giglio, J.-P. Muller, P. Lewis, and M. J. Barnsley, "The moderate resolution imaging spectroradiometer (MODIS): Land remote sensing for global change research," *IEEE Trans. Geosci. Remote Sensing*, vol. 36, pp. 1228–1249, July 1998.

[26] D. J. Diner, J. C. Beckert, T. H. Reilly, C. J. Bruegge, J. E. Conel, R. A. Kahn, J. V. Martonchik, T. P. Ackerman, R. Davies, S. A. W. Gerstl, H. R. Gordon, J.-P. Muller, R. B. Myneni, P. J. Sellers, B. Pinty, and M. M. Verstraete, "Multi-angle imaging spectroradiometer (MISR) instrument description and experiment overview," *IEEE Trans. Geosci. Remote Sensing*, vol. 36, pp. 1072–1085, July 1998.

[27] J. V. Martonchik, D. J. Diner, B. Pinty, M. M. Verstraete, R. B. Myneni, Y. Knyazikhin, and H. R. Gordon, "Determination of land and ocean reflective, radiative, and biophysical properties using multiangle imaging," *IEEE Trans. Geosci. Remote Sensing*, vol. 36, pp. 1266–1281, July 1998.

[28] E. F. Vermote, N. Z. El Saleous, and C. O. Justice, "Atmospheric correction of MODIS data in the visible to middle infrared: First results," *Remote Sens. Environ.*, 2002, to be published.

[29] O. Engelsen, B. Pinty, M. M. Verstraete, and J. V. Martonchik, "Parametric bidirectional reflectance factor models: Evaluations, improvements and applications," Presented at the Joint. Res. Cent. Eur. Comm., Ispra, Italy, Rep. EU 16426, 1996.

[30] J. V. Martonchik, "Determination of aerosol optical depth and land surface directional reflectances using multi-angle imagery," *J. Geophys. Res.*, vol. 102, pp. 17015–17022, 1997.

[31] A. Tarantola, *Inverse Problem Theory—Methods for Data Fitting and Model Parameter Estimation*. Amsterdam, The Netherlands: Elsevier Science, 1987.

[32] J. C. Price, "Comparison of the information content of data from the LANDSAT-4 thematic mapper and the multispectral scanner," *IEEE Trans. Geosci. Remote Sensing*, vol. 22, pp. 272–281, 1984.

[33] C. J. Bruegge, N. L. Chrien, R. R. Ando, and B. Chafin, "Ancillary radiometric product (ARP) usage in the EOS/MISR level 1B radiance product generation," in *Proc. SPIE, Earth Observing System, VI*,, vol. 4483, San Diego, CA, Aug. 2, 2001.

[34] S. Liang, H. Fang, M. Chen, C. J. Shuey, C. Walthall, C. Daughtry, J. Morisette, C. Schaaf, and A. Strahler, "Validating MODIS land surface reflectance and albedo products: Methods and preliminary results," *Remote Sens. Environ.*, 2002, to be published.

[35] D. W. Deering, T. F. Eck, and B. Banerjee, "Characterization of the reflectance aniostropy of three boreal forest canopies in spring-summer," *Remote Sens. Environ.*, vol. 67, pp. 205–229, 1999.

[36] D. J. Diner, G. P. Asner, R. Davies, Y. Knyazikhin, J.-P. Muller, A. W. Nolin, B. Pinty, C. B. Schaaf, and J. Stroeve, "New directions in earth observing: Scientific applications of multiangle remote sensing," *Bull. Amer. Meteorol. Soc.*, vol. 80, pp. 2209–2228, 1999.

[37] J. V. Martonchik, J. Hu, R. B. Myneni, Y. Knyazikhin, and D. J. Diner, "Surface reflectance and LAI/FPAR retrieval results from MISR," *IEEE Trans. Geosci. Remote Sensing*, to be published.

[38] J. V. Martonchik, D. J. Diner, R. A. Kahn, T. P. Ackerman, M. M. Verstraete, B. Pinty, and H. R. Gordon, "Techniques for the retrieval of aerosol properties over land and ocean using multiangle imaging," *IEEE Trans. Geosci. Remote Sensing*, vol. 36, pp. 1212–1227, July 1998.

Yufang Jin received the B.S. and M.S. degrees in atmospheric physics and environmental sciences from Peking University, Beijing, China, in 1995 and 1998, respectively. She is a Ph.D. candidate in geography at Boston University, Boston, MA, working on the evaluation of surface bidirectional reflectance and albedo retrievals from MODIS observations.

She was previously involved in applying atmospheric radiative transfer models for the retrieval of atmospheric aerosols from ground-based radiation and polarization measurements. Her research interests include earth's radiative energy budget, remote sensing of the atmosphere and the biosphere, and data assimilation in climate models.

Feng Gao (M'99) received the B.A. degree in geology and the M.S. degree in remote sensing from Zhejiang University, Hangzhou, China, in 1989 and 1992, respectively, and the Ph.D. degree in geography from Beijing Normal University, Beijing, China, in 1997.

From 1992 to 1998, he was a Research Scientist with the Nanjing Institute of Geography and Liminology, Chinese Academy of Science, Nanjing, China. Currently, he is a Research Assistant Professor with the Department of Geography and the Center for Remote Sensing, Boston University, Boston, MA. He is working on NASA's MODIS BRDF/Albedo project. His research interests include remote sensing modeling and retrieving vegetation parameters through inversion of BRDF models using directional measurements.

Crystal B. Schaaf (M'92) received the B.S. and M.S. degrees in meteorology from the Massachusetts Institute of Technology, Cambridge, in 1982, the M.L.A. degree in archaeology from Harvard University, Cambridge, MA, in 1988, and the Ph.D. degree in geography from Boston University, Boston, MA, in 1994.

She has been a research meteorologist with the USAF Phillips Laboratory, Hanscom, MA, specializing in remote sensing of clouds and the land surface. Currently, she is working as a Research Associate Professor of geography at Boston University for NASA's MODIS Project. Her research interests cover remote sensing of the biosphere and the atmosphere.

Xiaowen Li graduated from the Chengdu Institute of Radio Engineering, China, in 1968. He received the M.A. degree in geography, the M.S. degree in electrical and computer engineering, and the Ph.D. degree in geography from the University of California, Santa Barbara, in 1981 and 1985, respectively.

He is currently an academician at the Chinese Academy of Science, Nanjing, China, as a Professor and Director of the Research Center of Remote Sensing and GIS, as well as the Department of Geography, Beijing Normal University, Beijing, China. He is also a Research Professor at the Center of Remote Sensing and Department of Geography, Boston University, Boston, MA. His research interests are in 3-D modeling of reflectance and thermal emission of land surface, vegetation in particular, and information extraction from multiangular remote sensed images.

Alan H. Strahler (M'86) received the B.A. and Ph.D. degrees in geography from The Johns Hopkins University, Baltimore, MD, in 1964 and 1969, respectively.

He is currently a Professor of geography and a Researcher in the Center for Remote Sensing, Boston University, Boston, MA. He held a prior academic position at Hunter College of the City University of New York, New York, the University of California, Santa Barbara, and at the University of Virginia, Charlottesville. Originally trained as a biogeographer, he has been actively involved in remote sensing research since 1978. He has been a Principal Investigator on numerous NASA contracts and grants and is currently a member of the science team for the EOS MODIS instrument. His research interests are directed toward modeling the bidirectional reflectance distribution function (BRDF) of discontinuous vegetation covers and retrieving physical parameters describing ground scenes through inversion of BRDF models using directional radiance measurements. He is also interested in the problem of land cover classification using multitemporal, multispectral, multidirectional, and spatial information, as acquired in reflective and emissive imagery of the earth's surface.

Dr. Strahler was awarded the AAG/RSSG Medal for Outstanding Contributions to Remote Sensing in 1993.

Carol J. Bruegge received the B.A. and M.S. degrees in applied physics from the University of California, San Diego, in 1978 and the M.S. and Ph.D. degrees in optical sciences from the University of Arizona, Tucson, in 1985.

Currently, she is a Co-Investigator on the Multi-angle Imaging SpectroRadiometer (MISR) project and serves as the Calibration Scientist for that NASA Earth Observing System (EOS) instrument. Her experience is principally in the area of terrestrial remote sensing, calibration of remote sensing sensors, radiative transfer, and use of ground-truth measurements for validation and calibration of airborne and on-orbit sensors. She has been with the Jet Propulsion Laboratory, California Institute of Technology, Pasadena, CA, since 1985 and has been involved with the absolute radiometric calibration of the Landsat Thematic Mapper, AirMISR, and Airborne Visible and Infrared Imaging Spectrometer (AVIRIS) sensors. She has also provided for the flight qualification of Spectralon, a diffuse material now used on-orbit for the radiometric calibration of sensors. Previously, she has been a Principal Investigator in the First International Land Surface Climatology Program Field Experiment (FIFE), a NASA ground-truth experiment.

John V. Martonchik (A'01) received the B.S. degree in physics from Case Institute of Technology in 1964 and the Ph.D. degree in astronomy from the University of Texas, Austin, in 1974.

He is currently a Research Scientist at the Jet Propulsion Laboratory (JPL) and has been with JPL since 1972. His experiences include telescopic and spacecraft observations of planetary atmospheres, laboratory and theoretical studies of the optical properties of gaseous, liquid, and solid materials, and development and implementation of 1-D and 3-D radiative transfer and line-by-line spectroscopy algorithms for studies of planetary atmospheres and earth tropospheric remote sensing. He has been a Co-Investigator in several NASA programs and is the Algorithm Scientist for aerosol and surface retrievals on MISR.